Title

Demographic composition, not demographic diversity, predicts biomass and turnover across temperate and tropical forests

Journal

Global Change Biology, 28(9)

ISSN

1354-1013

Authors

Needham, Jessica F

Johnson, Daniel J

Anderson-Teixeira, Kristina J

et al.

Publication Date

2022-05-01

DOI

10.1111/gcb.16100

Peer reviewed

Demographic composition, not demographic diversity, predicts biomass and turnover across temperate and tropical forests

Running title: Demographic diversity of forests

Jessica F. Needham*[1,2,3], Daniel J. Johnson[4], Kristina J. Anderson-Teixeira[1,5], Norman Bourg[5], Sarayudh Bunyavejchewin[6], Nathalie Butt[7], Min Cao[8], Dairon Cárdenas[9], Chia-Hao Chang-Yang[10], Yu-Yun Chen[11], George Chuyong[12], Handanakere S. Dattaraja[13], Stuart J. Davies[1,14], Alvaro Duque[15], Corneille E. N. Ewango[16,17], Edwino S. Fernando[18], Rosie Fisher[20], Christine D. Fletcher[21], Robin Foster[22], Zhanqing Hao[23], Terese Hart[24], Chang-Fu Hsieh[25], Stephen P. Hubbell[26,27], Akira Itoh[28], David Kenfack[1,14], Charles D. Koven[3], Andrew J. Larson[29], James A. Lutz[30], William McShea[5], Jean-Remy Makana[17], Yadvinder Malhi[31], Toby Marthews[32], Mohizah Bt. Mohamad[33], Michael D. Morecroft[31], Natalia Norden[34], Geoffrey Parker[2], Ankur Shringi[13], Raman Sukumar[13,35], Hebbalalu S. Suresh[13,15], I Fang Sun[11], Sylvester Tan[33], Duncan W. Thomas[36], Jill Thompson[37], Maria Uriarte[38], Renato Valencia[39], T. L. Yao[21], Sandra L. Yap[40], Zuoqiang Yuan[41], Hu Yuehua[8], Jess K. Zimmerman[42], Daniel Zuleta[1,14], Sean M. McMahon[1,2]

Orchid IDs

Jessica F. Needham 0000-0003-3653-3848

Daniel J. Johnson 0000-0002-8585-2143

Kristina J. Anderson-Teixeira 0000-0001-8461-9713

Sarayudh Bunyavejchewin 0000-0002-1976-5041

Nathalie Butt 0000-0003-1517-6191

Min Cao 0000-0002-4497-5841

Chia-Hao Chang-Yang 0000-0003-3635-4946

Yu-Yun Chen 0000-0001-8760-8649

Edwino S. Fernando 0000-0001-9422-5451

Rosie Fisher 0000-0003-3260-9227

Chang-Fu Hsieh 0000-0003-4165-8100

Charles Koven 0000-0002-3367-0065

James A. Lutz 0000-0002-2560-0710

Toby Marthews 0000-0003-3727-6468

This article has been accepted for publication and undergone full peer review but has not been through the copyediting, typesetting, pagination and proofreading process, which may lead to differences between this version and the Version of Record. Please cite this article as doi: 10.1111/GCB.16100

Natalia Norden 0000-0001-5207-312X
I Fang Sun 0000-0001-9749-8324
Jill Thompson 000-0002-4370-2593
Renato Valencia 0000-0001-9770-6568
T. L. Yao 0000-0002-5274-1623
Jess K. Zimmerman 0000-0002-8179-0731
Daniel Zuleta 0000-0001-9832-6188
Sean McMahon 0000-0001-8302-6908

[1] Forest Global Earth Observatory
[2] Smithsonian Environmental Research Center, Edgewater, MD, USA
[3] Lawrence Berkeley National Laboratory, Berkeley, CA, USA
[4] School of Forest, Fisheries, and Geomatics Sciences, University of Florida, Gainesville, FL, USA
[5] Smithsonian Conservation Biology Institute, Front Royal, VA, USA
[6] Forest Research Office, Department of National Parks, Wildlife and Plant Conservation, Chatuchak, Bangkok, 10900, Thailand
[7] School of Earth and Environmental Sciences, University of Queensland, St Lucia, QLD 4072, Australia
[8] CAS Key Laboratory of Tropical Forest Ecology, Xishuangbanna Tropical Botanical Garden, Chinese Academy of Sciences, Kunming 650223, Yunnan, China
[9] Herbario Amazónico Colombiana, Instituto Amazónico de Investigaciones Científicas Sinchi, Bogotá, Colombia
[10] Department of Biological Sciences, National Sun Yat-sen University, Kaohsiung, Taiwan
[11] Department of Natural Resources and Environmental Studies, National Dong Hwa University, Hualien, Taiwan
[12] Department of Plant Science, University of Buea, Buea, Cameroon
[13] Centre for Ecological Sciences, Indian Institute of Science, Bangalore, Karnataka, India
[14] Smithsonian Tropical Research Institute, Washington DC, USA
[15] Departmento de Ciencias Forestales, Universidad Nacional de Colombia Sede Medellín, Medellín, Colombia
[16] University of Kisangani, Faculty of Sciences, Department of Plant Ecology & Natural Resources Management, Democratic Republic of Congo
[17] Centre de Formation et de Recherche en Conservation Forestière, Democratic Republic of Congo
[18] Department of Forest Biological Sciences, University of the Philippines, Los Baños, Philippines
[19] Institute of Biology, University of the Philippines – Diliman, Quezon City, Philippines

[20] National Center for Atmospheric Research, Boulder, CO, USA
[21] Forest Research Institute Malaysia, Kepong, 52109, Selangor, Malaysia
[22] Department of Botany, Field Museum, Chicago, IL, USA
[23] School of Ecology and Environment, Northwestern Polytechnical University, Xi'an, Shaanxi, China
[24] Tshuapa-Lomami-Lualaba Project (TL2), Democratic Republic of Congo
[25] Institute of Ecology and Evolutionary Biology, National Taiwan University, Taipei, Taiwan
[26] Department of Ecology and Evolutionary Biology, University of California, Los Angeles, CA, USA
[27] Smithsonian Tropical Research Institute, Panama City, Panama
[28] Graduate School of Science, Osaka City University, Osaka, Japan
[29] Department of Forest Management, W.A. Franke College of Forestry and Conservation, University of Montana, Missoula, MT, USA
[30] Wildland Resources Department, Utah State University, Logan, Utah, USA
[30] School of Geography and the Environment, University of Oxford, Oxford, UK
[32] UK Centre for Ecology & Hydrology, Wallingford, UK
[33] Sarawak Forestry Department, Kuching, Sarawak, Malaysia
[34] Programa de Ciencias Básicas de la Biodiversidad, Instituto de Investigación de Recursos Biológicos Alexander von Humboldt, Bogotá, Colombia
[35] Divecha Center for Climate Change, Indian Institute of Science, Bangalore, Karnataka, India
[36] School of Biological Sciences, Washington State University, Vancouver, WA, USA
[37] UK Centre for Ecology & Hydrology, Bush Estate, Penicuik, Midlothian, UK
[38] Department of Ecology, Evolution and Environmental Biology, Columbia University, New York, NY, USA
[39] Escuela de Ciencias Biológicas, Pontificia Universidad Católica del Ecuador, Quito, Ecuador
[40] Far Eastern University, Manila, Philippines
[41] Key Laboratory of Forest Ecology and Management, Institute of Applied Ecology, Chinese Academy of Sciences, Shenyang, China
[42] Department of Environmental Sciences, University of Puerto Rico, Río Piedras, Puerto Rico

*Corresponding author: jfneedham@lbl.gov, Present address: Lawrence Berkeley National Laboratory, Berkeley, CA, USA

Abstract

The growth and survival of individual trees determine the physical structure of a forest with important consequences for forest function. However, given the diversity of tree species and forest biomes, quantifying the multitude of demographic strategies within and across forests and the way that they translate into forest structure and function remains a significant challenge. Here, we quantify the demographic rates of 1,961 tree species from temperate and tropical forests and evaluate how demographic diversity (DD) and demographic composition (DC) differ across forests, and how these differences in demography relate to species richness, aboveground biomass, and carbon residence time. We find wide variation in DD and DC across forest plots, patterns that are not explained by species richness or climate variables alone. There is no evidence that DD has an effect on either aboveground biomass or carbon residence time. Rather, the DC of forests, specifically the relative abundance of large statured species, predicted both biomass and carbon residence time. Our results demonstrate the distinct demographic compositions of globally distributed forests, reflecting biogeography, recent history, and current plot conditions. Linking the demographic composition of forests to resilience or vulnerability to climate change, will improve the precision and accuracy of predictions of future forest composition, structure and function.

Key words: Aboveground biomass, Carbon residence time, Forest dynamics, ForestGEO, Size-dependent survival, Species richness, Tree demography

Introduction

Forests store approximately 50% of the world's carbon (Keenan & Williams 2018) and play a critical role in regulating the world's biogeochemical and hydrological cycles (Gloor et al. 2013). They cover 30% of the Earth's land surface and span vastly different environments. There are 50,000-80,000 tree species (Beech et al. 2017) and individual forest plots can vary in species richness by over three orders of magnitude (Anderson-Teixeira et al. 2015; Davies et al. 2021).

Tree species vary in their life histories, demographic rates and environmental specialization, yet within a forest, a diversity of life history strategies is not necessarily correlated with a diversity of species. Life-histories range from short-lived small understory species (Condit et al. 1994) to canopy species that reach 100 m in height (Koch et al. 2004; Sillett et al. 2010), or survive for thousands of years (Brokaw 1987; Chambers et al. 1998). Life histories can be specialized for specific environmental conditions, for example fast-growing pioneer species that occur in gaps (Brokaw 1987), and can have very different functional roles within the ecosystem in terms of carbon storage (Hubau et al. 2019; Lutz et al. 2018) and nutrient cycling (Ordoñez et al. 2009). Life history types may reflect strategies for dealing with forest perturbations,

and are expected to differ in their response to climate change and other global change factors (Phillips et al. 2002). Demographic rates form an important component of a species' overall life history strategy, reflecting the influence of both the environment and evolved strategies on the acquisition and allocation of resources. Greater species richness in the tropics, however, is not correlated with a greater range of growth and survival rates (Condit et al. 2006). Further, the biomass and turnover of forests do not show the same magnitude of variation as species richness (Lutz et al. 2018), suggesting a large degree of redundancy in the way that demographic rates of species scale to forest structure and function.

Demographic rates have typically been quantified by arranging species on the slow-fast continuum; an axis from slow-growing, long lived species to fast-growing, short-lived species (Wright et al. 2010). However, multiple species show demographic rates that do not align well with this single axis of demographic variation (Rüger et al. 2018, 2020; Russo et al. 2021). Further, the strength of the slow-fast continuum varies among forests, due to differences in environmental conditions (Russo et al. 2021). In highly disturbed forests the trade-off between growth and survival among species may be absent, as slow-growing, high survival species are never able to become established (Russo et al. 2021). Quantifying demographic diversity (DD), the range of demographic strategies, and demographic composition (DC), the relative abundance of different demographic strategies in a forest, therefore requires multiple axes of demographic variation (Rüger et al. 2018).

Here, we define the DD of a forest as the area occupied by species in demographic space - defined by multiple axes of demographic variation. Forests with high DD will have species with a wide range of growth and survival rates, whereas the species in forests with low DD will have a more limited range of growth and survival rates. We group species by demographic strategy through the use of clustering algorithms on species' positions in demographic space, and define the DC of a forest as the relative abundance of demographic strategies. Due to the ubiquity of gap-phase dynamics in closed-canopy forests (Brokaw 1987), we might expect to see some similarities in DC across forests, since all forests will contain demographic types specialized for different light conditions. However, it is not known whether the same strategies are comparable in absolute terms across forests, nor whether the proportions of demographic types vary across forests, or if particular demographic types are absent or overrepresented in some forests.

There are at least two hypotheses for how species richness might relate to forest biomass and carbon residence time via DD and DC, Fig. 1. First, higher species richness could lead to higher DD and aboveground biomass (AGB) because of niche-partitioning, where a more efficient use of resources would emerge from finer partitioning of resource space (Tilman et al. 1997). Second, the mass ratio hypothesis, first proposed by (Grime 1998), suggests that observed patterns of AGB relate not to the number of species, but rather to the demographic rates of dominant species in the forest community. In this case, species richness may be unrelated to DD and AGB, as it is the presence or absence of species with particular demographic strategies (i.e., forest DC), which define the structure and functioning of the forest. A

number of features unique to a location, such as seasonality, recent land use history, geophysical features, biogeography, and disturbance regimes could all shape DC. The relationship between carbon residence time and species richness, DD, and DC is more complex as it depends on both AGB and AGB loss from mortality. Under the niche-complementarity hypothesis higher species richness would lead to higher DD and AGB but either lower or higher mortality rates, depending on the increase in demographic diversity. As a result, carbon residence times would likely increase, but in some cases could decrease. Under the mass ratio hypothesis, AGB and AGB losses from mortality have no relationship with species richness and DD, and therefore carbon residence time would be defined by the dominant species, rather than species diversity.

Although a number of studies have addressed aspects of demography and diversity either directly (e.g., Condit et al. 2006; Rüger et al. 2020), or indirectly through the effects of mechanisms on demographic rates (e.g., Comita et al. 2010), the majority of studies have focused on distinct biomes, and have not incorporated forests across orders of diversity, with distinct floras, and unique climate and disturbance regimes.

Here, we quantify the diversity of demographic rates across temperate and tropical forests in an effort to understand the extent to which demographic strategies explain how forests that exhibit conspicuously different species richness vary in terms of AGB and turnover, and how this relates to climatic conditions. We ask (1) How much does DD vary among forests around the world and how does species richness correlate with demographic diversity? (2) How do forests differ in DC i.e., how do the proportions of demographic strategies differ across forests? (3) How are DD and DC related to environmental conditions? And (4) How are DD and DC related to AGB and carbon residence time?

Methods

Plots and data

We used demographic data from 20 plots across the ForestGEO network of permanent forest plots ((Davies et al. 2021), https://forestgeo.si.edu, [Fig. S1]). Plots span a latitudinal gradient from the most equatorial at 0° 69 ' S (Yasuní Ecuador) to the most northerly at 51°77 ' N (Wytham, UK). Data collection at each plot follows a standardised protocol

described in Condit (1998), where every stem ≧ 1 cm DBH (diameter at breast height, 1.3 m above the ground) is measured, mapped, and identified to species. Censuses are typically carried out every five years. For this analysis, we used one census interval from every plot (see Table S1). In order to have sufficient sample sizes, we limited our analysis to species with at least 200 individuals. In highly diverse or relatively small plots, this threshold means that many rare species were excluded from the analysis. However, due to highly skewed species abundance distributions, the percentage of stems included in the analysis ranged from 45% to 98% across plots, with a mean of 84% of stems included. Tree ferns, palms, lianas and bamboos were also excluded due to non-standard growth forms. In total, the data set includes 2,195,135 stems of 1,961 species. For further details of each plot see Table S1. Although some of the plots experience disturbance, there were no major cyclones or droughts at any of the plots between the two censuses that we used in this analysis.

Statistical Analysis

Survival

We simultaneously fitted separate size-dependent survival curves to small and large stems, using a common asymptote, so that survival probability was a smooth function of stem size.

We modelled size dependent survival probability across a census interval, as:

$$s = \left(\frac{K}{1 + (e^{-r_1(z-p_1)})}\right)^t \text{ for all } z < c$$

$$s = \left(\frac{K}{1 + (e^{-r_2(z-p_2)})}\right)^t \text{ for all } z \geq c$$

Eq. 1

where z is DBH in mm and K is the upper asymptote of the curves and represents maximum survival, often constant across much of the DBH range, *r* is a rate parameter that determines the rate of survival increases (r_1) or decreases (r_2) with size, and *p* is the inflection point, i.e., the size at which survival probability is 0.5. Subscripts 1 and 2 denote the parameters for the survival curves at sizes below and above the DBH threshold where the curves meet, *c*. We set *c* to 0.2 * max(DBH) to ensure sufficient individuals above and below the DBH threshold. Raising to the power *t*, the time in years between censuses, makes parameters describe the annual probability of survival. For all further analysis, we used maximum survival (MS) (usually, but not always K), and juvenile survival (JS) - the survival probability at 10 mm DBH.

Although we refer to this as juvenile survival, in some species individuals may already be several decades old and reproductive at 10 mm DBH, the smallest size in the inventory data.

Growth

To account for negative growth in the census data, which may result from measurement error, stem damage or differences in water content, from one census to the next, we adapted the method described by (Rüger et al. 2011). We resampled all stem measurements 1000 times according to the distribution sda + sdb x dbh, where sda = 0.927 mm and sdb = 0.0038 mm. If any increments were still negative, we assigned a growth increment by sampling from the positive growth increments in the plot.

We divided individuals of each species at a given plot into the slowest growing 95% of the population and the fastest 5% of the population and fit Gamma distributions to the DBH increment data for each group separately. The Gamma distribution has the flexibility to capture both the highly skewed distribution of slow growth and the more symmetric distribution of faster growth:

$$\Delta z \sim \begin{cases} \text{Gamma}(\alpha_1, \beta_1) \text{ for } \Delta z < q \\ \text{Gamma}(\alpha_2, \beta_2) \text{ for } \Delta z \geq q. \end{cases} \quad \text{Eq. 2}$$

Delta *z* is the absolute annual change in DBH in mm, alpha and beta are the shape and rate parameters of the Gamma distribution respectively and *q* is the percentile determining the proportion of individuals in the fast growth distribution, here the 95% percentile of DBH increment. Subscripts 1 and 2 denote growth distributions fit to individuals with growth below and above *q*, respectively. In further analyses, we used the expectation of growth (in mm yr^{-1}), given by alpha/beta for the slow and fast growth distribution for each species, hereafter 95G and 5G.

We estimated growth and survival parameters using Bayesian Markov Chain Monte Carlo (MCMC) with the *rstan* package (Stan Development Team 2016) in R (R Core Team 2021). For each species, we ran three chains with 2,500 iterations and checked diagnostic plots for convergence. For further details of the growth and survival models see Needham et al. (2018).

We did not include reproduction in these analyses due to a lack of data at the global scale. In several studies, (e.g., Rüger et al. 2020; Salguero-Gómez et al. 2016), recruitment into a census is used as a proxy for reproductive effort. However, in our study, which includes all species with a DBH of 1 cm, recruitment into a census does not have a consistent interpretation across species. For example, a 1 cm DBH stem could be a reproductive stem of an adult shrub

species, or a non-reproductive juvenile sapling of a canopy species. We therefore chose to focus our analysis on growth and survival, which better capture forest biomass and turnover across life-history strategies.

Principal Component Analysis (PCA)

To identify orthogonal axes of demographic variation, we performed a PCA on the growth and survival parameters for each species at each plot. We used logistic transformations of MS and JS (to improve normality), and non-transformed 5G and 95G. We also included the maximum DBH for each species, denoted ST. We used the PCA function from the *FactoMineR* R package (Lê et al. 2008) as it allowed us to weight species by the inverse of the number of plots they occur in, preventing species with wider geographic distributions having disproportionate influence on the results (115 species (5.9%) occurred in more than one plot). We did not attempt a phylogenetically controlled PCA due to the lack of well resolved phylogeny for the majority of species in our analysis. Incorrect tree topologies, along with incomplete taxon sampling, would introduce biases into any estimation of a phylogenetic signal in demographic rates (Ackerly 2000; Symonds 2002). All PCA axes are shown in Fig. S2.

Demographic Diversity Across Plots

To address question one, we calculated the DD of each plot as the convex hull of species from that plot along the first two dimensions of PCA space, which together explain 76.2% of variation in growth and survival among plots (Cornwell et al. 2006) (Fig. 3). We scaled the coordinates of each species along each axis by the percentage variation explained by that axis. We then plotted DD and species richness across plots and fitted a spline through the data using the ss function of the npreg package in R (Helwig 2021) (Fig. 4). As a measure of the degree of demographic similarity among plots, we calculated the pairwise overlap of convex hulls (Fig. S3). To account for different plot sizes, we randomly sampled 500 bootstrap samples of 400 20 m x 20 m quadrats (equivalent to the size of the smallest plot, 16 ha) from each plot with replacement. For each unique bootstrapped sample, we calculated the species richness and then calculated the convex hull for those species present in the sampled 16 ha. We present here the mean number of species with ≥ 200 individuals across samples as species richness, the mean convex hull volume as DD, the median area of overlap from pairwise overlaps of 500 convex hulls at each plot for similarity in DD. In all but one plot (BCI), all species with over 200 individuals in the full data set were found in all 500 bootstrap samples. Convex hulls and overlaps were calculated using the geometry package in R (Habel et al. 2019).

Demographic Composition Across Plots

To address question two, we first clustered species into demographic types, or specifically, growth-survival-stature modes (GSSMs), based on similarities in observed demographic rates. To determine the similarities in demographic rates we used the position of each species in multi-dimensional PCA space using the clustering kmeans function in base R (R Core Team 2021), with 200 starting points. The *kmeans* function minimises the sum of squares from each species to the centre of its assigned GSSM. Using 200 starting points allows the algorithm to explore multiple centres for each GSSM and thus optimises clustering. We tested different combinations of clustering algorithms and cluster numbers (Figs. S4, S5), and identified eight GSSMs that were biologically interpretable (Fig. 2) and that met statistical standards in cluster analysis: high Dunn index, low number of negative silhouettes, no cluster with too few species, and high explained variance (Figs. S4, S5). For each plot we calculated the relative abundance of each GSSM as a measure of demographic composition (Fig. S6). We then tested whether DC was correlated with species richness across plots (Fig S7). Our third question was how are DD and DC related to environmental conditions? We therefore tested whether DD and DC at each plot are predicted by mean annual temperature (MAT) and mean annual precipitation (MAP), taken from Anderson-Teixeira et al. (2015) (Figs 5, S8, S9). We did not correct for multiple hypotheses related to the relative abundance of GSSMs and MAT, MAP, and species richness, as we are more interested in the relationship between each GSSM and each variable (see (Cabin and Mitchell 2000) for discussions of the problems with Type II errors in ecological studies). We present Rsq and p-values but avoid significance testing and discuss inference using the language of 'evidence' as discussed in Muff et al. (2021).

To explore differences in life histories across GSSMs, we calculated passage times and life expectancies for each GSSM using a simple individual based model (IBM). For each GSSM we found the mean growth and survival parameters from all species in that GSSM. We simulated 25000 individuals until all individuals had died. Five percent of individuals grew according to the fast growth distribution, and 95% according to the slow growth distribution (eq 2). Survival was a draw from a binomial distribution each year with probabilities given by the size-dependent function described in eq 1. We calculated life expectancies as the mean time to death for a 10 mm DBH stem, and passage times as the mean time taken to grow from 10 mm DBH to 100 mm DBH (a size that all GSSMs can reach), conditional on survival.

Aboveground Biomass Across plots

Our final question was how do DD and DC vary with AGB and carbon residence across plots? To test this, we estimated AGB and carbon residence time at each plot. We estimated AGB using equations and parameters from Chave et al. (2014) for tropical plots and from Jenkins et al. (2003) and Chojnacky et al. (2014) for temperate plots. We calculated AGB for all stems in each plot using the following equations.

For tropical plots, we calculated AGB as:

$$AGB = exp[-1.803 - 0.976E + 0.976ln(wsg) + 2.673ln(D) - 0.0299[ln(D)]^2]$$ Eq. 3

where D is DBH in cm, wsg is wood specific gravity and E is a local bioclimatic variable (Chave et al. 2014). *wsg* estimates come from Zanne et al. (2009), see Chave et al. (2009). We use species level estimates of *wsg* where available, and genus, family or global means depending on availability. Values of E for each plot come from http://chave.ups-tlse.fr/pantropical_allometry.htm. E is defined as

$$E = 1.e - 3 * (0.178 * TS - 0.938 * CWD - 6.61 * PS)$$ Eq. 4

where TS is temperate seasonality as defined in the Worldclim dataset (bioclimatic variable 4). CWD is climatic water deficit and PS is precipitation seasonality as defined in the Worldclim dataset (bioclimatic variable 15). Higher values of E result in lower estimates of AGB. For more details see http://chave.ups-tlse.fr/pantropical_allometry.htm.

For temperate plots, we calculated AGB as:

$$AGB = exp[\beta_0 + \beta_1 ln(D)]$$ Eq. 5

We used parameter values from Chojnacky et al. (2014) which depend on wood specific gravity. Again, these come from Zanne et al. (2009), see Chave et al. (2009).

Aboveground Carbon Residence Time

We calculated aboveground carbon residence time at each plot as AGB / AGB_{mort}, where AGB_{mort} is AGB loss from mortality, following Koven et al. (2015). For AGB_{mort} we followed Sullivan et al. (2020) , to take into account unobserved growth of trees present at the first census that had died by the second census, and recruits that entered during a census interval but died before being recorded in the second census. The unobserved growth of trees that died, and unobserved recruits were estimated from per area annual recruitment and per-capita annual mortality using equations 11 and 5 from Kohyama et al. (2017). For more information see SI Methods S1. We tested the correlations between AGB and

carbon residence time with DD. We further tested for correlations between AGB and carbon residence time with the relative abundance of each GSSM (Fig. 6, S10, S11). Again, we present tests independently, but follow Moffit et al. and discuss our findings in terms of 'evidence'.

Results

Axes of demographic variation

The first Principal Component (PC) accounts for 49% of the variation among species (Table 1), and corresponds to a trade-off between growth and juvenile survival (Fig. 2, growth rates [both 95G and 5G], as growth and juvenile survival rates [JS] have opposite loadings on the first axis). Maximum survival (MS) is largely orthogonal to growth rates. The positive loadings of both 95G and 5G on PC 1 suggests that species are generally consistently fast-growing or slow-growing, i.e., if the fastest 5% of the population (5G) are fast-growing then the slowest 95% of the population (95G) are also relatively fast-growing. PC 2 explains 27.2% of variation and describes an axis associated with low survival and small stature at one extreme and high survival and large stature at the other. Other axes are shown in Fig. S2. Species are not evenly distributed across the growth-survival space, but are clustered in regions of high survival and slow growth. GSSM 2, a slow-growing, small-statured and low survival mode, had the most species, 29%, followed by GSSM 1, 23%, a very slow-growing, high-survival mode.

Demographic diversity shows a complex association with species richness

Our first question asked how DD varies among forests and whether species richness correlates with DD. We estimated DD at each plot by calculating the area of the convex hull around species' positions in PCA space (Fig. 3). We find that DD varies widely across plots and initially shows a steep increase with increasing species richness (Fig. 4). DD increases from low to intermediate levels of species richness and is roughly level at high species richness plots.

Demographic composition varies across forests

Our second question asked how DC varies across plots. We compared where species from each plot are located in PCA space (Fig. 2), the pairwise overlap of plots in PCA space (Fig. S3), as well as the relative abundance of GSSMs at each plot (Fig. S6). Communities of species from each plot occupy different regions of PCA space (Fig. 3) with some clustered in regions of high survival, and others more spread out to include fast growing species. Tropical plots have a higher degree of overlap with other plots, due to higher species richness and larger convex hulls. BCI (Panama), La Planada (Colombia) and other plots with fast growing species have the greatest degree of overlap with other plots (Fig. S3). We

found moderate evidence for an effect of species richness on the relative abundance of GSSM 6 (Rsq = 0.29, p = 0.018), but weak or no evidence of species richness having an effect on the relative abundance of any other GSSM (Fig. S7). There is little evidence for an effect of species richness on the relative abundance of GSSM 6 among tropical plots (Rsq = 0.11, p = 0.24). The relationship between species richness and the relative abundance of GSSM 6 is driven by the inclusion of temperate plots.

Climate variables predict demographic diversity and composition

Our third question asked how DD and DC are related to environmental conditions. We find strong evidence that DD increases with increasing mean annual temperature (MAT) (Rsq = 0.43, p = 0.0022), but this correlation is mostly driven by a clear trend in temperate plots (Fig. 5), and therefore would be unlikely to confirm a causal relationship from temperature to DD globally. Among tropical plots, there is no evidence for an effect of MAT on DD (Rsq = 0.002, p = 0.88). We also find no evidence of an effect of mean annual precipitation (MAP) on DD (Rsq = 0.14, p = 0.11). There is strong evidence that the relative abundance of the large statured growth-survival-stature mode (GSSM) 6 decreases with increasing MAT (Rsq = 0.48, p = 0.00094). Again, this correlation is mostly driven by the inclusion of temperate plots that contain a greater proportion of large statured species, given their lower species diversity. Small-statured, high-survival GSSM 2 has a positive correlation with MAT (Rsq = 0.32, p = 0.012), as does large statured, fast growing GSSM 7 (Rsq = 0.2, p = 0.058). There is moderate evidence that GSSM 3 is positively correlated with MAP (Rsq = 0.28, p = 0.02) and GSSM 6 negatively correlated with MAP (Rsq = 0.23, p = 0.039). Otherwise, there is weak or no evidence for an effect of MAT or MAP on any other GSSM (Figs S8 and S9).

Demographic composition, not diversity, predicts forest structure

Our final question asked how DD and DC are related to AGB and carbon residence time. We find no evidence that DD is related to either AGB or carbon residence time across plots (Rsq = 0.014, p = 0.63; Rsq = 0.15, p = 0.12) (Fig. 6). We find strong evidence that the relative abundance of GSSM 5 is positively correlated with AGB (Rsq = 0.33, p = 0.0095), and moderate evidence that the relative abundance of GSSM 6 is correlated with carbon residence time (Rsq = 0.23, p = 0.043), even when we remove Wytham Wood, which had a carbon residence time more than double that of any other plot.

Discussion

We fitted growth and survival models to 1,961 species from twenty temperate and tropical forests and assessed global patterns of demographic diversity (DD) and demographic composition (DC). While DD initially increases with species richness it levels off in high diversity plots and there is no evidence of a relationship with either AGB or carbon residence time. In contrast, we find strong evidence for a relationship between DC and AGB, specifically for an increase in AGB with an increase in the relative abundance of large statured demographic types, and moderate evidence that DC has an effect on carbon residence time across forests.

Demographic diversity has a complex association with species richness

Our first question was how does DD vary among forests around the world and are species rich forests more demographically diverse? We find wide variation in DD across forests, but a complex association between species richness and DD. DD initially increases with increasing species richness but peaks at intermediate levels of species richness and reaches a plateau across highly species rich plots (Fig. 4). Condit et al. (2006) similarly found that across ten tropical forests the most species rich forests had the lowest demographic diversity. This might be due to the fact that, in species rich tropical forests an increase in species richness does not necessarily translate to an increase in richness at higher taxonomic levels, rather, particular genera are highly species-rich (Davies et al. 2005), (Richardson et al. 2001). If so, this accumulation of species within genera could introduce demographic redundancy; explaining the plateau reached after intermediate levels of species richness. Because demographic rates within many species-rich tropical tree genera tend to be phylogenetically conserved, additional species do not always increase the demographic diversity of the forest (Davies et al. 2005). More information on the similarity of demographic rates among closely related species could provide insights into the mechanisms that determine DD across forests.

The relationship between demographic diversity and species richness also likely relates to disturbance regimes. Highly disturbed plots in our analysis (e.g., HKK (Thailand), Palanan (Philippines), Fushan (Taiwan), and Luquillo (Puerto Rico))

tend to have lower species richness than less disturbed sites. Yet despite having fewer species, disturbed sites have high DD due to greater numbers of fast-growing species, which can capitalize on increased light availability and nutrients generated by disturbance (Brokaw 1987). Since variation in growth rates is larger than variation in survival rates, plots with high disturbance rates have higher DD by our measure because they contain species located on the edge of PCA space towards very fast growth. Examples include HKK (Thailand), a seasonally dry forest with frequent ground fires, and Palanan (Philippines), a cyclone prone forest. In contrast, plots that have relatively low DD but high species richness, such as Lambir (Malaysia), are dominated by slow growing, high survival species. This is likely due to exceptionally low soil fertility, which also limits growth (Russo et al. 2005). Our results are in line with findings from Russo et al. (2021) who found that in highly disturbed plots the strength of the growth-survival trade-off is weaker than in relatively stable undisturbed plots because slow-growing, high-survival species are not able to become established (Russo et al. 2021). Quantifying disturbance rates is challenging due to the variability in disturbance regimes and the difficulty in quantifying disturbance across many forests. For instance, disturbances affecting forests in this study include elephants, wildfires, cyclones and windthrows. Estimating disturbance intensity at a given site is challenging, as intensity can vary greatly over small spatial scales due to topographical heterogeneity, wind exposure (Negrón-Juárez et al. 2014) and soil saturation (Margrove et al. 2015). In many cases the best indicator of the severity of a disturbance is mortality rates. Our results suggest that disturbances may be a key driver of demographic differences across sites, making this an important area of future research.

Demographic composition varies across forests

Since we are interested in the role that demography plays in shaping the AGB and turnover of forests, we also explored differences in DC across plots. We find that despite the diversity of forest types included in our study, many of the same demographic strategies are present across forests (Fig. S6). This may be partially due to physiological constraints on tree life-history. Although tree life-history strategies can be very varied, growth and survival of trees is relatively limited compared with the differences in demographic rates across the whole plant kingdom (Salguero-Gómez et al. 2016). In most forests, there are canopy and understory species with a range of growth and survival rates. Yet, differences in biogeography and environmental conditions alter the relative abundance of demographic types, with consequences for vertical forest structural complexity and the strength of demographic trade-offs (Russo et al. 2021).

One important difference among forests in terms of DC is the relative abundance of large statured species, which is highest in forests with low species richness (Fig. S7). This finding is in agreement with previous work across temperate and tropical plots (Lutz et al. 2018) and can be explained by the greater structural complexity of tropical forests. Due to limited space in the canopy, high stem density in tropical forests is normally associated with an increase in canopy layers and higher numbers of small-statured understory individuals (Bohlman & Pacala 2012; Farrior et al. 2016). Increased

subcanopy layers lead to a decrease in the relative abundance of large canopy trees, even if the absolute abundance remains the same. Why there is such a diversity of subcanopy species in some tropical forests, as opposed to a high stem density of fewer species, remains unanswered, although one hypothesis is that greater niche complementarity in the tropics allows for a higher number of species to coexist (Chesson et al. 2013; Loreau 1998).

There is moderate evidence for a relationship between climate variables and demographic diversity and demographic composition

To better understand the mechanisms driving differences in demography across forests, we tested for correlations between climate variables, and both DD and DC. Demographic rates have been shown to correlate with climate variables at the regional and pan-tropical scale (Esquivel-Muelbert et al. 2020; Johnson et al. 2018). Most notably, annual growth rates are slower at higher latitudes with lower temperatures. While we also find evidence of a correlation between temperature and DD, there is no evidence for such a relationship within the tropics (Fig. 5). Survival rates within the tropics decreases with increasing aridity, e.g. (Locosselli et al. 2020), yet we find no evidence of an effect of mean annual precipitation on DD, possibly because DD is also defined by growth rates and stature in our analysis, which may show little correlation with precipitation. DC is mostly unrelated to temperature and precipitation, with the exception that the relative abundance of large-statured species decreases with increasing MAT. These correlations are likely driven by the strong increase in species richness with MAT, which as noted above, leads to greater structural complexity and a decrease in the relative abundance of large canopy trees. Our results suggest that, while DD and DC show some correlation with climate, the dynamics at a particular plot cannot be predicted by these metrics alone.

Demographic composition, not diversity, predicts forest structure

In answer to our fourth question, we find evidence that DC, but not DD, is related to AGB and carbon residence time (Fig. 6). Despite species richness varying by nearly 60 times, the two highest biomass plots in our study are Lambir, a dipterocarp forest in Malaysian Borneo, and Wind River, a temperate forest in the Pacific Northwest of the USA that is dominated by *Tsuga heterophylla* (western hemlock), and *Pseudotsuga menziesii* (Douglas-fir). Our results highlight that there are multiple ways to be a high biomass forest, from species rich, tropical forests, to temperate forests dominated by just a handful of species. Both Lambir and Wind River are dominated by species in GSSMs 5 and 6, demographic types characterised by large stature. In Lambir just 26% of individuals, but 75% of AGB is in GSSMs 5 and 6, whereas in Wind River 78% of individuals and 98% of AGB is in GSSMs 5 and 6. Our results support previous findings that the maximum height of dominant species, rather than a diversity of functional traits, determines biomass across forests (Finegan et al. 2015; Van Pelt et al. 2016). Our results suggest that species identity, rather than species richness or DD, determines carbon dynamics.

Aboveground carbon residence time, here defined as the length of time that carbon remains in living, aboveground tissue of trees, is strongly influenced by the growth and mortality of individual trees. Together growth and survival rates determine how quickly carbon is accumulated and how long that carbon is stored. Differences in growth and survival rates among GSSMs results in passage times that range from means of 15 to 151 years, and life expectancies that range from mean of 17 to 87 years (Fig. S13). Despite small stature, GSSM 1 had the longest mean life expectancy (87 years) due to the slow growth and high survival of species in this mode. This finding is in line with previous studies that have shown that understory trees make substantial contributions to carbon storage in African forests (Hubau et al. 2019). Disturbances lead to higher mortality and thus decrease carbon residence time (e.g. Gora et al. 2020). Increases in disturbance frequency could directly decrease carbon residence time through short-term increases in mortality, but also indirectly through shifts in composition towards demographic types with faster growth rates and higher mortality.

Conclusions and future directions

Here we have presented a quantitative analysis of the relationship between species richness, demography, and forest structure and turnover. While we find little evidence for an effect of DD on AGB or carbon residence time, an important question that remains unanswered is whether forests that are more demographically diverse will show greater resilience to future perturbations. Many combinations of functional traits can give rise to the same demographic rates. As a result, species with similar demographic rates may respond differently to disturbance, and a forest with a high degree of demographic redundancy could be buffered from disturbance if some of the species are themselves resilient, or the mixture of species confers resilience. As disturbances are predicted to increase in the future (McDowell et al. 2020), it is important to explore the extent to which DD and DC determine forest response to changes in disturbance frequency and intensity. This may be especially important with regards to large trees. Our results highlight the importance of large-statured trees for forest ecosystem function across temperate and tropical regions. Shifts in DC following changes to disturbance regimes could have significant consequences for AGB and carbon residence time if they result in a decrease in the abundance of large statured demographic types. An improved understanding of the determinants of DC across forests will be essential to predict forest response to future climates and disturbance regimes.

Tables

Table 1. Variable loadings, eigenvalues and percent variance explained by each PCA axis.

	PC 1	PC 2	PC 3	PC 4	PC 5
MS	-0.24	0.84	0.27	-0.41	-0.01
JS	-0.63	0.52	0.13	0.57	0.01
ST	0.57	0.61	-0.54	0.04	0.07
95G	0.89	0.04	0.36	0.13	0.22
5G	0.93	0.15	0.14	0.12	-0.27
Eigenvalue	2.45	1.36	0.54	0.52	0.13
% variance	48.97	27.22	10.79	10.45	2.56
Cumulative % variance	48.97	76.19	86.98	97.44	100

Data Availability Statement

Data is available from https://www.forestgeo.si.edu or from the authors upon request. R scripts for analyzing the data and producing the figures in the paper are available from Jessica Needham's GitHub at https://github.com/JessicaNeedham/ForestGEO_global_demography.

Acknowledgements

SMM was partially funded by the USA National Science Foundation (NSF 640261 to SMM). This project began and was developed at ForestGEO workshops in 2016, 2017 and 2018 (NSF DEB-1046113 to S.J. Davies). For individual plot acknowledgements see SI. We acknowledge the contributions of Dr. Perry Ong and Dr. Abdul Rahman to the Palanan and Pasoh projects respectively.

Conflict of interest

The authors declare no conflict of interest.

Bibliography

Ackerly DD. 2000. Taxon sampling, correlated evolution, and independent contrasts. *Evolution*. 54(5):1480–92

Anderson-Teixeira KJ, Davies SJ, Bennett AC, Gonzalez-Akre EB, Muller-Landau HC, et al. 2015. CTFS-ForestGEO: a worldwide network monitoring forests in an era of global change. *Glob. Chang. Biol.* 21(2):528–49

Beech E, Rivers M, Oldfield S, Smith PP. 2017. GlobalTreeSearch: The first complete global database of tree species and country distributions. *Journal of Sustainable Forestry*. 36(5):454–89

Bohlman S, Pacala S. 2012. A forest structure model that determines crown layers and partitions growth and mortality rates for landscape-scale applications of tropical forests. *Journal of Ecology*. 100(2):508–18

Brokaw NVL. 1987. Gap-Phase Regeneration of Three Pioneer Tree Species in a Tropical Forest. *J. Ecol.* 75(1):9

Chambers JQ, Higuchi N, Schimel JP. 1998. Ancient trees in Amazonia. *Nature*. 391(6663):135–36

Chave J, Coomes D, Jansen S, Lewis SL, Swenson NG, Zanne AE. 2009. Towards a worldwide wood economics spectrum. *Ecol. Lett.* 12(4):351–66

Chave J, Réjou-Méchain M, Búrquez A, Chidumayo E, Colgan MS, et al. 2014. Improved allometric models to estimate the aboveground biomass of tropical trees. *Glob. Chang. Biol.* 20(10):3177–90

Chesson P, Pacala S, Neuhauser C. 2013. *10. Environmental Niches and Ecosystem Functioning*. Princeton University Press

Chojnacky DC, Heath LS, Jenkins JC. 2014. Updated generalized biomass equations for North American tree species. *Forestry*. 87(1):129–51

Comita LS, Muller-Landau HC, Aguilar S, Hubbell SP. 2010. Asymmetric density dependence shapes species abundances in a tropical tree community. *Science*. 329(5989):330–32

Condit R, Ashton P, Bunyavejchewin S, Dattaraja HS, Davies S, et al. 2006. The importance of demographic niches to tree diversity. *Science*. 313(5783):98–101

Condit R, Hubbell SP, Foster RB. 1994. Density dependence in two understory tree species in a neotropical forest. *Ecology*. 75(3):671–80

Condit R. 1998. The CTFS and the standardization of methodology. In *Tropical Forest Census Plots*, pp. 3–7. Berlin, Heidelberg: Springer Berlin Heidelberg

Cornwell WK, Schwilk LDW, Ackerly DD. 2006. A trait-based test for habitat filtering: convex hull volume. *Ecology*. 87(6):1465–71

Davies SJ, Abiem I, Abu Salim K, Aguilar S, Allen D, et al. 2021. ForestGEO: Understanding forest diversity and dynamics through a global observatory network. *Biological Conservation*. 253:108907

Davies SJ, Tan S, LaFrankie JV, Potts MD. 2005. Soil-Related Floristic Variation in a Hyperdiverse Dipterocarp Forest. In *Pollination Ecology and the Rain Forest*, eds. DW Roubik, S Sakai, AA Hamid Karim, pp. 22–34. New York: Springer-Verlag

Esquivel-Muelbert A, Phillips OL, Brienen RJW, Fauset S, Sullivan MJP, et al. 2020. Tree mode of death and mortality risk factors across Amazon forests. *Nat. Commun.* 11(1):5515

Farrior CE, Bohlman SA, Hubbell S, Pacala SW. 2016. Dominance of the suppressed: Power-law size structure in tropical forests. *Science*. 351(6269):155–57

Finegan B, Peña-Claros M, de Oliveira A, Ascarrunz N, Bret-Harte MS, et al. 2015. Does functional trait diversity predict above-ground biomass and productivity of tropical forests? Testing three alternative hypotheses. *J. Ecol.* 103(1):191–201

Gloor M, Brienen RJW, Galbraith D, Feldpausch TR, Schöngart J, et al. 2013. Intensification of the Amazon hydrological cycle over the last two decades. *Geophys. Res. Lett.* 40(9):1729–33

Gora EM, Burchfield JC, Muller-Landau HC, Bitzer PM, Yanoviak SP. 2020. Pantropical geography of lightning-caused disturbance and its implications for tropical forests. *Glob. Chang. Biol.* 26(9):5017–26

Grime JP. 1998. Benefits of plant diversity to ecosystems: immediate, filter and founder effects. *Journal of Ecology*. 86(6):902–10

Habel K, Grasman R, Gramacy RB, Mozharovskyi P, Sterratt DC. 2019. geometry: Mesh Generation and Surface Tessellation. *R package version 0.4.5*

Helwig NE. 2021. npreg: Nonparametric Regression via Smoothing Splines. R package version 1.0-6. *CRAN R project*

Hubau W, De Mil T, Van den Bulcke J, Phillips OL, Angoboy Ilondea B, et al. 2019. The persistence of carbon in the African forest understory. *Nat. Plants*. 5(2):133–40

Jenkins JC, Chojnacky DC, Heath LS, Birdsey RA. 2003. National scale biomass estimators for United States tree species. *Forest Science. 49: 12-35*

Johnson DJ, Needham J, Xu C, Massoud EC, Davies SJ, et al. 2018. Climate sensitive size-dependent survival in tropical trees. *Nat. Ecol. Evol.* 2(9):1436–42

Keenan TF, Williams CA. 2018. The terrestrial carbon sink. *Annu. Rev. Environ. Resour.* 43(1):219–43

Koch GW, Sillett SC, Jennings GM, Davis SD. 2004. The limits to tree height. *Nature*. 428(6985):851–54

Kohyama TS, Kohyama TI, Sheil D. 2017. Definition and estimation of vital rates from repeated censuses: Choices, comparisons and bias corrections focusing on trees. *Methods Ecol. Evol.*

Koven CD, Chambers JQ, Georgiou K, Knox R, Negron-Juarez R, et al. 2015. Controls on terrestrial carbon feedbacks by productivity versus turnover in the CMIP5 Earth System Models. *Biogeosciences*. 12(17):5211–28

Lê S, Josse J, Husson F. 2008. FactoMineR : An *R* package for multivariate analysis. *J. Stat. Softw.* 25(1):

Locosselli GM, Brienen RJW, Leite M de S, Gloor M, Krottenthaler S, et al. 2020. Global tree-ring analysis reveals rapid

decrease in tropical tree longevity with temperature. *Proc Natl Acad Sci USA*. 117(52):33358–64

Loreau M. 1998. Biodiversity and ecosystem functioning: a mechanistic model. *Proc Natl Acad Sci USA*. 95(10):5632–36

Lutz JA, Furniss TJ, Johnson DJ, Davies SJ, Allen D, et al. 2018. Global importance of large-diameter trees. *Global Ecol. Biogeogr.*

Margrove JA, Burslem DFRP, Ghazoul J, Khoo E, Kettle CJ, Maycock CR. 2015. Impacts of an extreme precipitation event on dipterocarp mortality and habitat filtering in a bornean tropical rain forest. *Biotropica*. 47(1):66–76

McDowell NG, Allen CD, Anderson-Teixeira K, Aukema BH, Bond-Lamberty B, et al. 2020. Pervasive shifts in forest dynamics in a changing world. *Science*. 368(6494):

Muff S, Nilsen EB, O'Hara RB, Nater CR. 2021. Rewriting results sections in the language of evidence. *Trends Ecol. Evol.*

Needham J, Merow C, Chang-Yang C-H, Caswell H, McMahon SM. 2018. Inferring forest fate from demographic data: from vital rates to population dynamic models. *Proc. Biol. Sci.* 285(1874):

Negrón-Juárez R, Chambers J, Hurtt G, Annane B, Cocke S, et al. 2014. Remote Sensing Assessment of Forest Disturbance across Complex Mountainous Terrain: The Pattern and Severity of Impacts of Tropical Cyclone Yasi on Australian Rainforests. *Remote Sens (Basel)*. 6(6):5633–49

Ordoñez JC, van Bodegom PM, Witte J-PM, Wright IJ, Reich PB, Aerts R. 2009. A global study of relationships between leaf traits, climate and soil measures of nutrient fertility. *Global Ecology and Biogeography*. 18(2):137–49

Phillips OL, Vásquez Martínez R, Arroyo L, Baker TR, Killeen T, et al. 2002. Increasing dominance of large lianas in Amazonian forests. *Nature*. 418(6899):770–74

Richardson JE, Pennington RT, Pennington TD, Hollingsworth PM. 2001. Rapid diversification of a species-rich genus of neotropical rain forest trees. *Science*. 293(5538):2242–45

Rüger N, Berger U, Hubbell SP, Vieilledent G, Condit R. 2011. Growth strategies of tropical tree species: disentangling light and size effects. *PLoS ONE*. 6(9):e25330

Rüger N, Comita LS, Condit R, Purves D, Rosenbaum B, et al. 2018. Beyond the fast-slow continuum: demographic dimensions structuring a tropical tree community. *Ecol. Lett.* 21(7):1075–84

Rüger N, Condit R, Dent DH, DeWalt SJ, Hubbell SP, et al. 2020. Demographic trade-offs predict tropical forest dynamics. *Science*. 368(6487):165–68

Russo SE, Davies SJ, King DA, Tan S. 2005. Soil-related performance variation and distributions of tree species in a Bornean rain forest. *Journal of Ecology*. 93(5):879–89

Russo SE, McMahon SM, Detto M, Ledder G, Wright SJ, et al. 2021. The interspecific growth-mortality trade-off is not a general framework for tropical forest community structure. *Nat. Ecol. Evol.* 5(2):174–83

Salguero-Gómez R, Jones OR, Jongejans E, Blomberg SP, Hodgson DJ, et al. 2016. Fast-slow continuum and reproductive strategies structure plant life-history variation worldwide. *Proc Natl Acad Sci USA*. 113(1):230–35

Sillett SC, Van Pelt R, Koch GW, Ambrose AR, Carroll AL, et al. 2010. Increasing wood production through old age in tall

trees. *Forest Ecology and Management*. 259(5):976–94

Sullivan MJP, Lewis SL, Affum-Baffoe K, Castilho C, Costa F, et al. 2020. Long-term thermal sensitivity of Earth's tropical forests. *Science*. 368(6493):869–74

Symonds MRE. 2002. The effects of topological inaccuracy in evolutionary trees on the phylogenetic comparative method of independent contrasts. *Syst. Biol.* 51(4):541–53

Tilman D, Lehman CL, Thomson KT. 1997. Plant diversity and ecosystem productivity: theoretical considerations. *Proc Natl Acad Sci USA*. 94(5):1857–61

Van Pelt R, Sillett SC, Kruse WA, Freund JA, Kramer RD. 2016. Emergent crowns and light-use complementarity lead to global maximum biomass and leaf area in Sequoia sempervirens forests. *Forest Ecology and Management*. 375:279–308

Wright SJ, Kitajima K, Kraft NJB, Reich PB, Wright IJ, et al. 2010. Functional traits and the growth-mortality trade-off in tropical trees. *Ecology*. 91(12):3664–74

Zanne AE, Lopez-Gonzalez G, Coomes DA, Ilic J, Jansen S, et al. 2009. Data from: Towards a worldwide wood economics spectrum. *Dryad Digital Repository*

Fig 1. Conceptual model of the relationship between species richness, demographic diversity (DD), and aboveground biomass (AGB). In the niche complementarity hypothesis (top row) species have different resource requirements resulting in different demographic rates (a). (b) shows the position of species in demographic space, defined by demographic rates, with DD depicted as the yellow convex hull around species, and demographic composition (DC) shown by clusters of species in different colours. As species richness increases more resources are used resulting in higher DD, DC and AGB (c). Alternatively, in the mass ratio hypothesis (bottom row), species may overlap in their resource usage (d). Increasing species richness, therefore, does not necessarily result in greater DD or DC (e). Under this hypothesis, AGB is defined by the presence or absence of large statured species, i.e., by demographic composition. DD, DC and AGB may have no relationship with species richness.

Fig. 2 Growth-survival state space Principal component analysis and clustering analysis on growth and survival parameters for 1,961 species across twenty tropical and temperate forests. Parameters are described in detail in the main text. PC 1 corresponds to a trade-off between growth and juvenile survival and accounts for 49.0% of the variation among species. PC 2 accounts for 27.2% of variation and is a stature and survival axis, characterised by high maximum survival and large stature at one extreme and low maximum survival and small stature at the other. We used clustering algorithms to group species into eight 'growth-survival-stature modes' (GSSMs), depicted with different colours and given a number from 1-8.

Fig. 3 Position of plots in growth-survival space. Position of species in the first two dimensions of demographic space for each plot sorted from left to right, top to bottom by latitude (plots on the bottom row are temperate plots). Grey dots show species from all plots, coloured dots indicate the species from the named plot, with lines connecting each species to the community centroid. Shading shows the demographic diversity of each plot, calculated as the convex hull area for species from each plot.

Fig. 4 Relationship between species richness and demographic diversity. Species richness here is the mean number of species with over 200 individuals found in 500 bootstrap samples of 16 ha from each plot. To estimate demographic diversity, we calculated the volume of the convex hull of species along the first two axes of the growth-survival PCA for each bootstrap sample of species richness. Units of demographic diversity thus refer to the PCA axes. We fit a spline through the data using the *ss* function from the *npreg* package in R. Demographic diversity increases from low to moderate levels of species richness and is roughly level at high species richness. Note that the x-axis is logged for visualisation purposes.

Fig. 5 Correlation between climate variables and both demographic diversity and the relative abundance of large statured species. Mean annual temperature (MAT) and mean annual precipitation (MAP) are taken from Anderson-

Teixiera (2015). Growth survival stature mode (GSSM) 6 is the demographic type characterised by fast growing large statured species. Demographic diversity (DD) is the volume of the convex hull around species from each plot in the first two dimensions of PCA space. There is strong evidence for DD increasing with increasing MAT (Rsq = 0.43, p = 0.002). However, within the tropics, there is no evidence that MAT has an effect on DD (Rsq = 0.002, p = 0.88). There is very strong evidence that the relative abundance of GSSM 6 decreases with MAT (Rsq = 0.48, p = 0.00095), but weak evidence for an effect of MAP on the relative abundance of GSSM 6 (Rsq = 0.23, p = 0.039). For the effect of climate variables on other GSSMs see Figs S8 and S9.

Fig. 6 Demographic diversity (DD) versus aboveground biomass (AGB) and carbon residence time. DD is the volume of the convex hull around species from each plot in the first two dimensions of PCA space. In panels d,e and f) Wytham Woods is excluded from the analysis (but shown in the figure) due to its very high carbon residence time of 347 years. There is no evidence that DD has an effect on either AGB or carbon residence time (Rsq = 0.014, p = 0.63; Rsq = 0.15, p = 0.12). There is strong evidence that the relative abundance of growth-survival-stature-mode (GSSM) 5 has an effect on AGB (Rsq = 0.33, p = 0.0095). There is moderate evidence that the relative abundance of GSSM 6 has an effect on carbon residence time (Rsq = 0.23, p = 0.043).

(a)
Low species richness
High species richness
Resource 2
Resource 1
(b)
Low species richness
High species richness
Demographic axis 2
Demographic axis 1
(c)
DD DC AGB
Species Richness
(d)
Low species richness
High species richness
Resource 2
Resource 1
(e)
Low species richness
High species richness
Demographic axis 2
Demographic axis 1
(f)
DD DC AGB
Species Richness

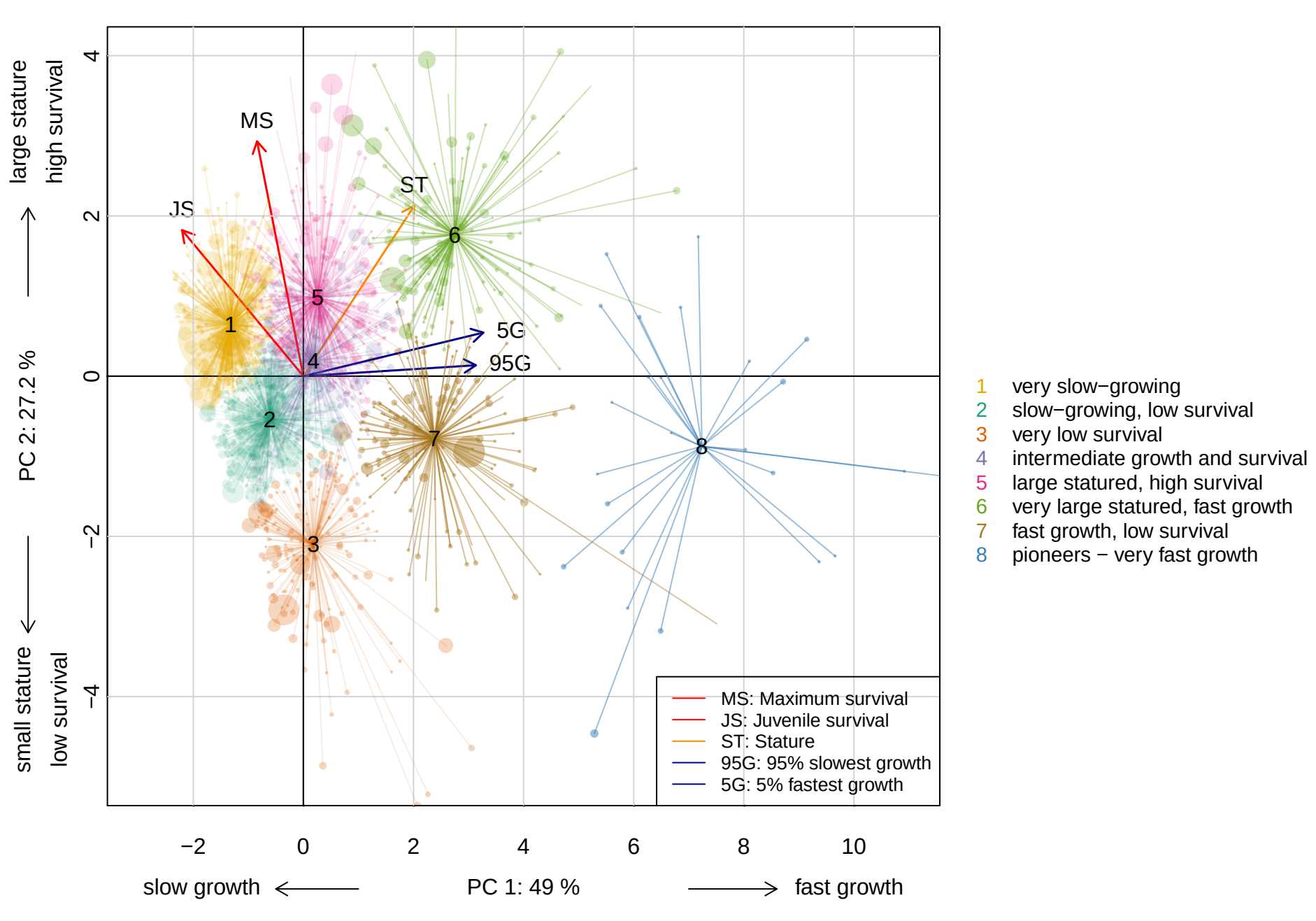
large stature
high survival
small stature
low survival
PC 2: 27.2 %
slow growth
PC 1: 49 %
fast growth
MS
JS
ST
5G
95G
1
2
3
4
5
6
7
8
MS: Maximum survival
JS: Juvenile survival
ST: Stature
95G: 95% slowest growth
5G: 5% fastest growth
1 very slow−growing
2 slow−growing, low survival
3 very low survival
4 intermediate growth and survival
5 large statured, high survival
6 very large statured, fast growth
7 fast growth, low survival
8 pioneers − very fast growth

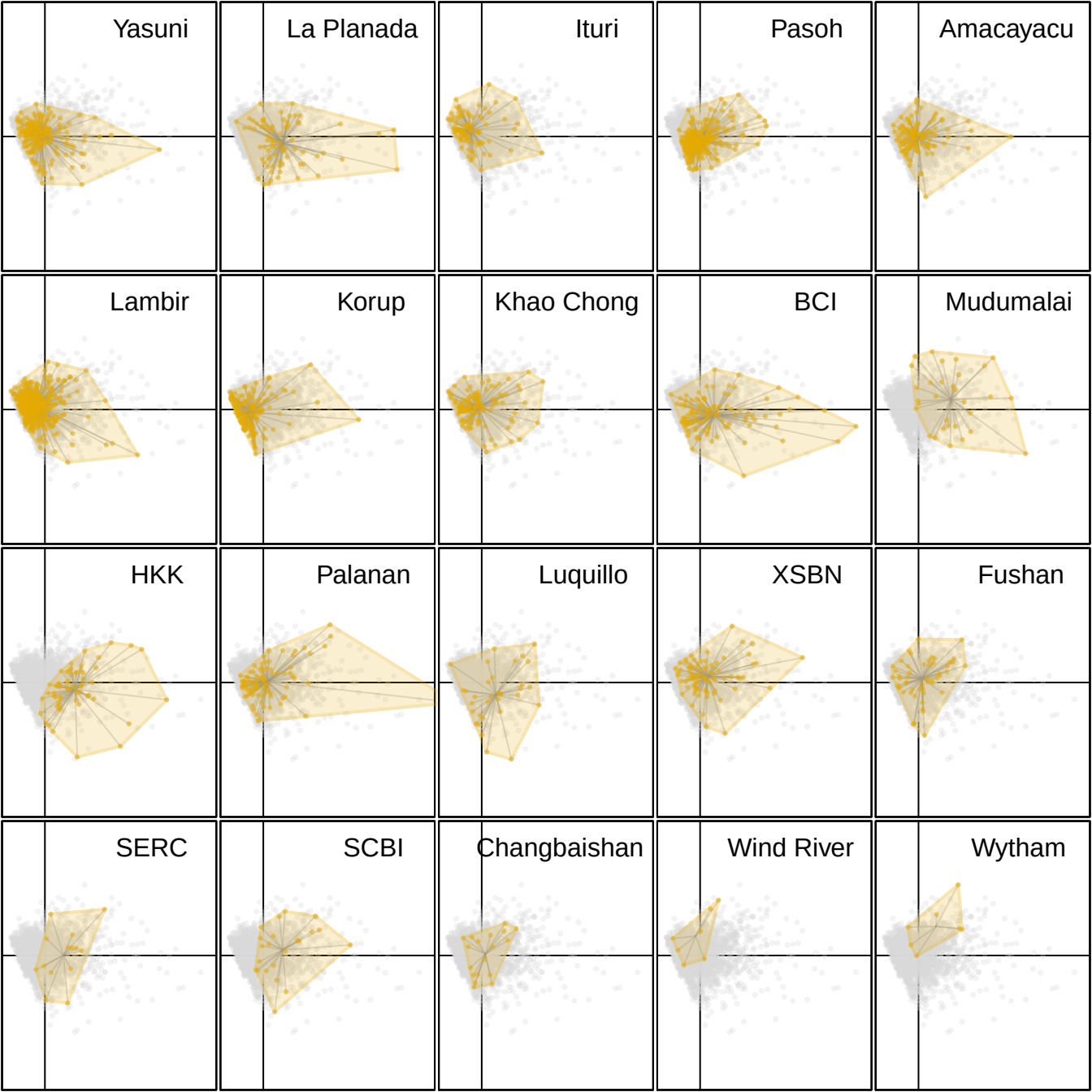
Yasuni
La Planada
Ituri
Pasoh
Amacayacu
Lambir
Korup
Khao Chong
BCI
Mudumalai
HKK
Palanan
Luquillo
XSBN
Fushan
SERC
SCBI
Changbaishan
Wind River
Wytham

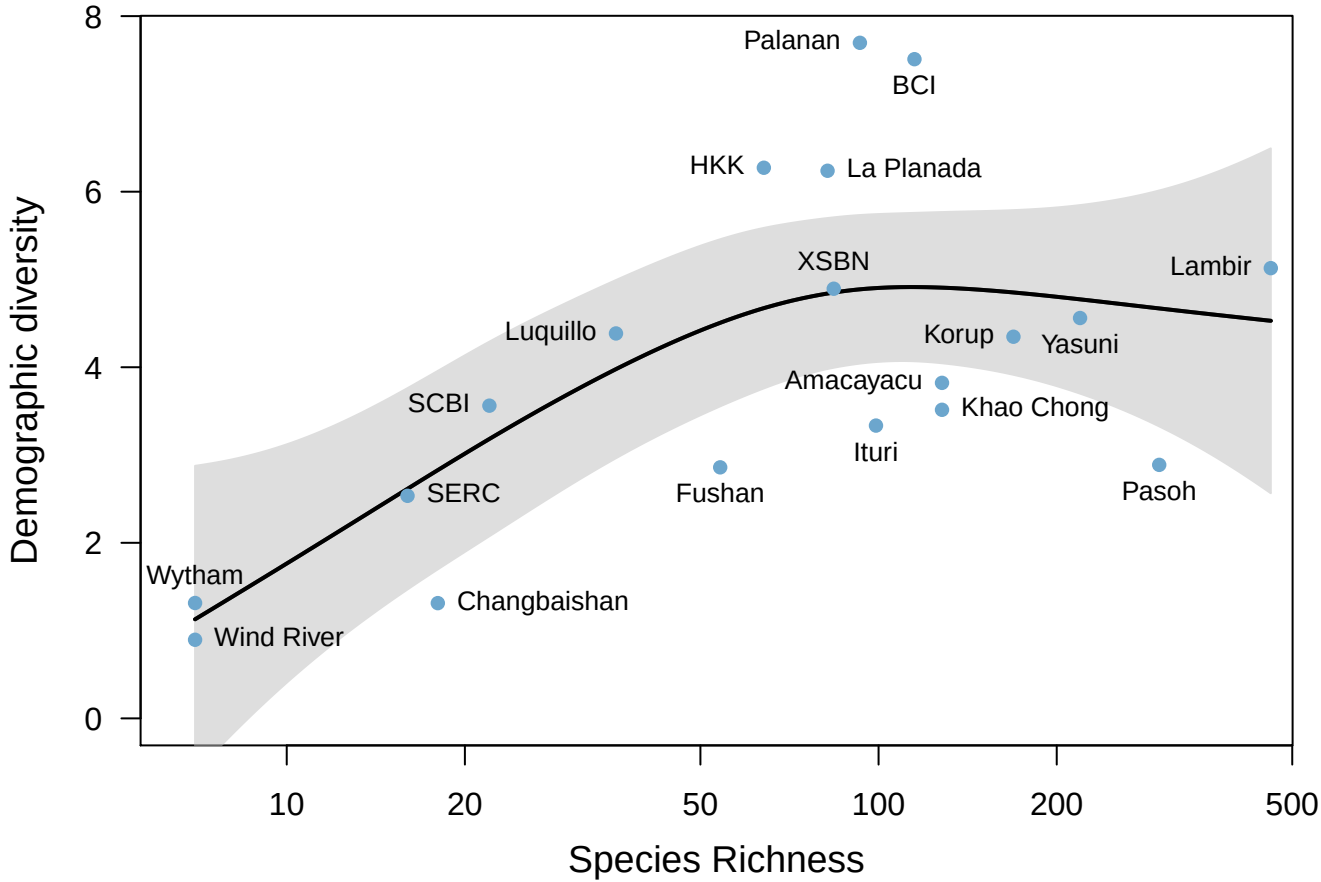
Demographic diversity
Species Richness
0
2
4
6
8
10
20
50
100
200
500
Palanan
BCI
HKK
La Planada
XSBN
Lambir
Luquillo
Korup
Yasuni
Amacayacu
SCBI
Khao Chong
Ituri
SERC
Fushan
Pasoh
Wytham
Changbaishan
Wind River

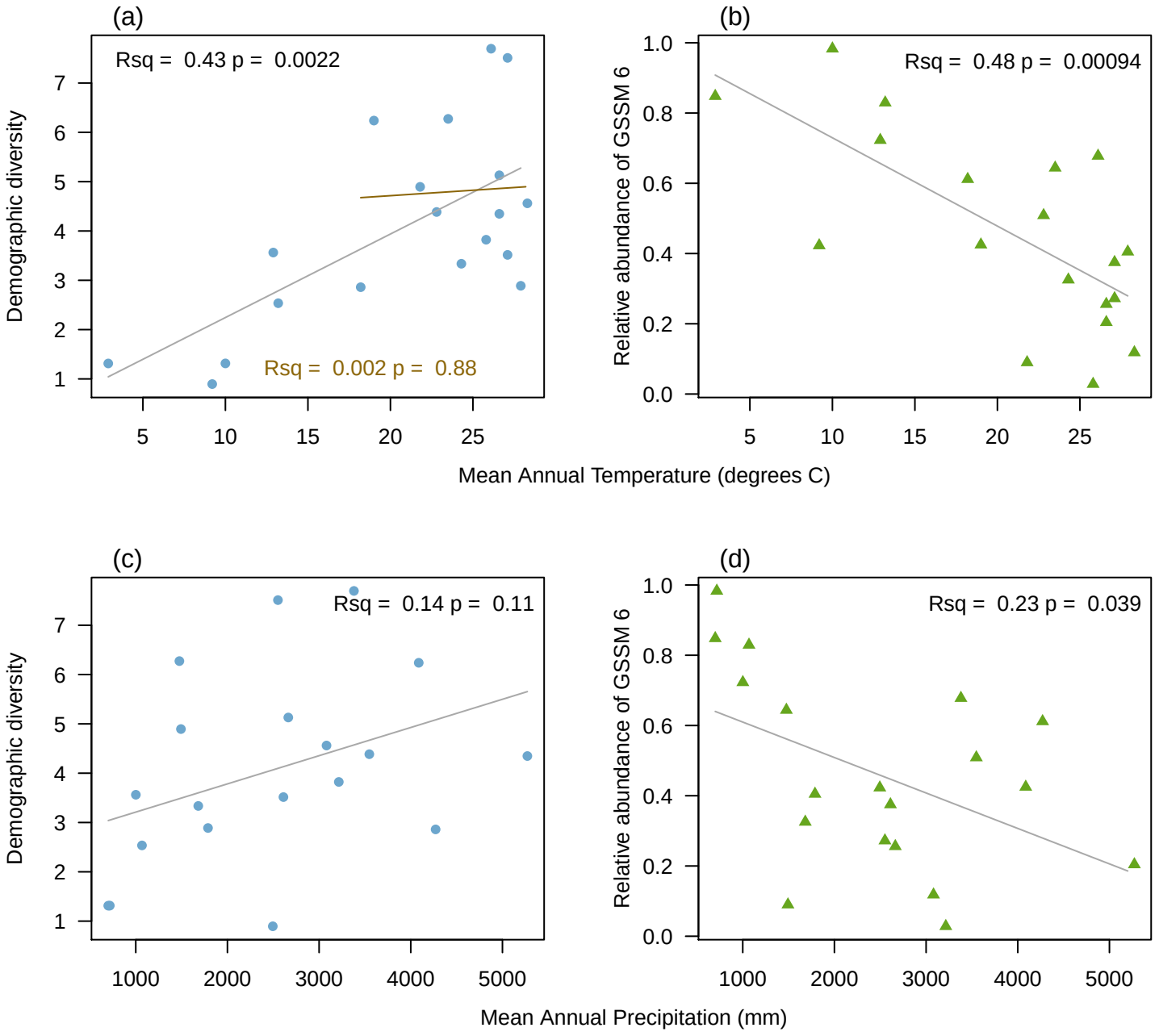
(a)
Rsq = 0.43 p = 0.0022
Rsq = 0.002 p = 0.88
Demographic diversity
(b)
Rsq = 0.48 p = 0.00094
Relative abundance of GSSM 6
Mean Annual Temperature (degrees C)
(c)
Rsq = 0.14 p = 0.11
Demographic diversity
(d)
Rsq = 0.23 p = 0.039
Relative abundance of GSSM 6
Mean Annual Precipitation (mm)

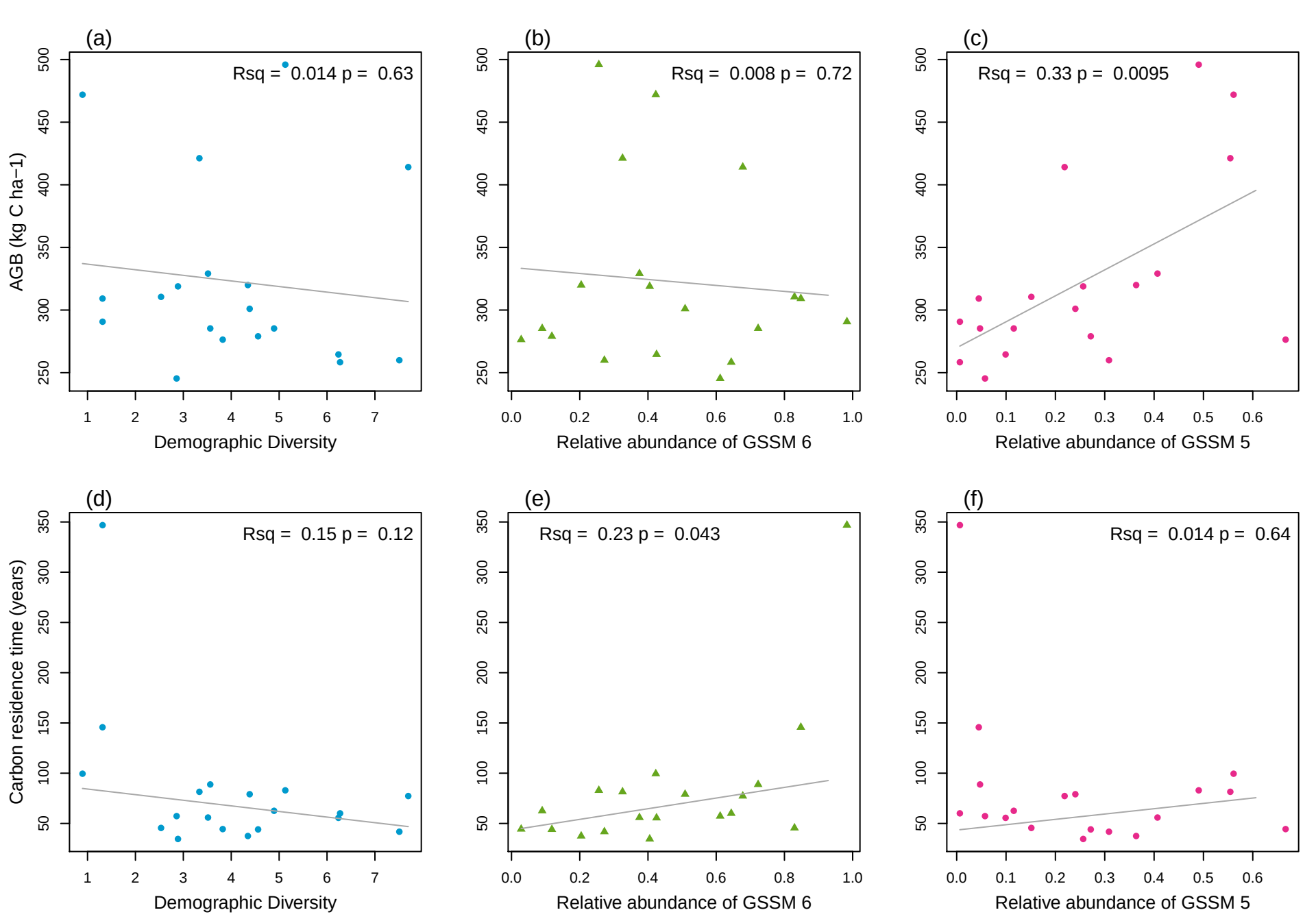
(a)
Rsq = 0.014 p = 0.63
AGB (kg C ha−1)
Demographic Diversity
(b)
Rsq = 0.008 p = 0.72
Relative abundance of GSSM 6
(c)
Rsq = 0.33 p = 0.0095
Relative abundance of GSSM 5
(d)
Rsq = 0.15 p = 0.12
Carbon residence time (years)
Demographic Diversity
(e)
Rsq = 0.23 p = 0.043
Relative abundance of GSSM 6
(f)
Rsq = 0.014 p = 0.64
Relative abundance of GSSM 5